Spatial Correlations in Finite Samples Revealed by Coulomb Explosion

Ulf Saalmann, Alexey Mikaberidze,[*] and Jan M. Rost

Max Planck Institute for the Physics of Complex Systems, Nöthnitzer Straße 38, 01187 Dresden, Germany
(Received 24 December 2012; published 25 March 2013)

We demonstrate that fast removal of many electrons uncovers initial correlations of atoms in a finite sample through a pronounced peak in the kinetic-energy spectrum of the exploding ions. This maximum is the result of an intricate interplay between the composition of the system from discrete particles and its boundary. The formation of the peak can be described analytically, accounting for correlations beyond a mean-field reference model. It can be experimentally detected with short and intense light pulses from 4th-generation light sources.

PACS numbers: 36.40.Gk, 79.77.+g

Correlation effects beyond the mean-field description are important in understanding the detailed structure of matter. A major scheme has been the "exchange-correlation hole" indispensable in electronic-structure theory [1], which focuses on bound states, mostly even on the ground state. Nowadays, very intense laser pulses at extreme ultraviolet and x-ray energies [2,3] can create situations which allow us to probe correlations in the continuum. One phenomenon in this context is massively parallel ionization [4] of a cluster or large molecule: Many electrons are ionized almost simultaneously to an energy high enough that the attractive ionic background does not play a role in the short time span during which energy exchange of electrons in the continuum happens.

Complementarily, one may ask how the many ions behave, whose dynamics (in the case of short intense x-ray pulses [2,3]) develops on a longer time scale, when most of the electrons have left [5]. Do the ions also develop a correlated motion in the continuum—and if so, what are its characteristics in terms of observables, e.g., the energy spectrum of the ions? The simplest description well known from plasma physics approximates these ions as a continuous charge density. The corresponding spectrum provides a comparison for highlighting the differences to a correlated continuum calculation. They occur for two reasons: first, the granularity of our system, i.e., the fact that we deal with real particles which typically have a minimal separation δ and therefore give rise to a classical "correlation hole." Moreover, the ionic system is finite (for simplicity, we assume a spherical shape) with an edge. The softness of this edge, i.e., the distance a over which the charge density decreases to zero, is the second spatial scale which influences the ionic correlations in the continuum. In fact, we will show that the ion dynamics exhibits a crossover, characterized by the ratio a/δ, from a dominant influence of the correlation hole if $a \ll \delta$ (hard edge) to the dominant influence of the edge for $a \gg \delta$ (soft edge).

Surprisingly, this crossover can be probed by simply varying the pulse length of the ionizing light pulse in the correct parameter regime: A long pulse (for reasonable target systems this would be of the order of a few hundred femtoseconds) will slowly ionize the cluster and give the ions created near the surface time to move outward. Thereby, a soft edge in terms of decreasing density of ions is created. On the other hand, a short violent pulse (of a few femtoseconds only) will start the motion of all ions created at once leading to correlation-hole dominated dynamics.

Whereas most cluster experiments at the x-ray free-electron lasers [3] address xenon clusters [6,7], mainly because of the large scattering cross sections, or argon clusters [8], because of the internal electron dynamics [9], the correlation effect discussed in the following would be most easily identified experimentally with ultrashort pulses and low-Z clusters.

We set the stage by defining the mean-field reference system, a homogeneously charged sphere of charge Q and mass M. It undergoes Coulomb explosion, doubling its initial radius R in time [10]

$$t_\star = (1 + \ln(\sqrt{2} + 1)/\sqrt{2})\sqrt{MR^3/Q^2}. \qquad (1)$$

Making use of Gauss' law and the fact that shells of charge in a homogeneously charged sphere do not overtake each other, one can directly map the initial potential energy due to the enclosed charge at a radius r to the final kinetic energy E per unit charge $E(r) = Qr^2/R^3$. Evaluating the standard expression for the energy distribution

$$\frac{dP}{dE} = \frac{3}{R^3} \int_0^R dr\, r^2 \delta(E - E(r)) \qquad (2)$$

yields [12–14]

$$\frac{dP}{dE} = \begin{cases} (3/2)\sqrt{E/E_\star^3} & \text{for } E < E_\star \\ 0 & \text{for } E > E_\star, \end{cases} \qquad (3a)$$

$$E_\star = Q/R. \qquad (3b)$$

In terms of these scales for energy $E_\star$ and time $t_\star$, we show in Fig. 1 kinetic-energy spectra of ions from Lennard-Jones (LJ) clusters [15] with 1000 particles for various effective pulse duration T. Hereby, effective pulse duration refers to
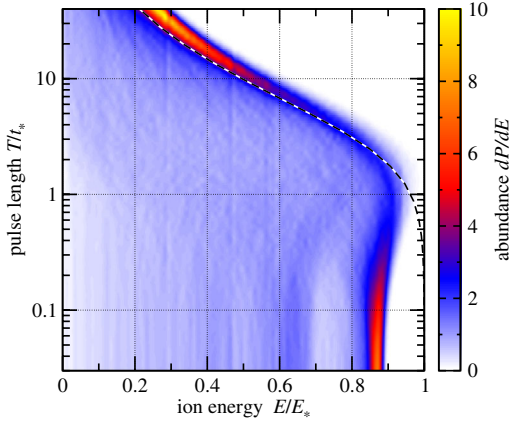
FIG. 1 (color online).   Ion-energy spectra as obtained from an
exploding LJ cluster with 1000 particles for various pulse
durations T given in units of the expansion time $t_\star$, cf. Eq. (1).
Energy is given in terms of $E_\star$ the highest energy for homoge-
neously charged sphere, cf. Eq. (3b). The dashed line marks the
surface energy of a sphere, which is charged homogeneously
according to a Gaussian pulse (see text).

the time in which the particles get charged. We select
randomly a charging time for each particle in such a way
that the ensemble averaged charge grows as $\langle Q_t \rangle = Q[1 +
\mathrm{erf}(t/T)]/2$ which, e. g., corresponds to ionization of atoms
in a cluster by single-photon ionization, as it would occur
for a sample exposed to intense free-electron laser radia-
tion with keV photons in a Gaussian pulse [16]. At such
photon energies electrons are "kicked out" so quickly that
their impact on the ion dynamics can be safely neglected.

One clearly sees in Fig. 1 a crossover behavior with two
"hot spots" at short and long pulses [cf. also Fig. 2(a)]
which shows the height of the ridge as a function of pulse
length T], always close to the maximal energy possible
at a given pulse length T. The long-pulse regime is com-
patible with a mean-field dominated dynamics and has
been described previously: This mean-field peak in the
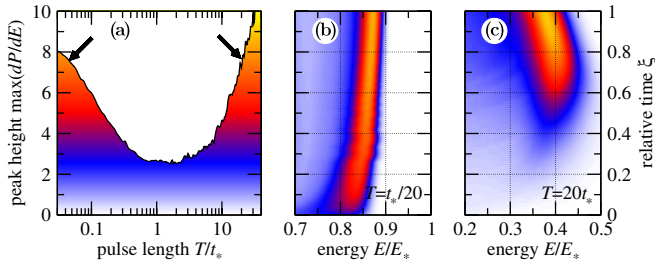
FIG. 2 (color online).   Peak height of kinetic-energy spectra for
ions shown in Fig. 1 for different pulse lengths $T/t_\star$ (a). The two
arrows indicate the pulse lengths $T = t_\star/20$ and $T = 20t_\star$ for
which the evolution of the spectra dP/dE are shown in (b) and
(c), respectively, as a function of energy and time $\xi \in [0, 1]$. The
time variable $\xi = E(t)/E(\infty)$ describes how far the Coulomb
explosion has evolved in terms of the kinetic energy $E(t)$ of an
expanding homogeneously charged sphere.

kinetic-energy spectrum was observed for spherical objects
with a washed-out edge, i.e., a nonuniform radial density
distribution. It allows faster ions from inner regions of an
exploding sample to overtake slower outer ones, leading to
radial caustics, as revealed by means of a kinetic model
[17]. Under suitable conditions this caustic can even lead to
a shock shell [13]. Preexploding the sample [18] softens
the edge of the system to a gradually decreasing density,
which is indeed close to the situation for long pulses shown
in Fig. 1. Charging at low densities as effected by a long
laser pulse reduces the energy deposition in the sample
and leads to a global decrease of kinetic energies for long
pulses, also visible in the spectrum for a homogeneously
charged sphere (dashed line in Fig. 1).

What has not been seen before is the sharp maximum for
short pulses whose origin is fundamentally different from
the *mean-field peak* at long pulses. We will refer to this
maximum as the *granularity peak* since its origin is the
granularity of the system in connection with the fact that
it is finite and has an edge. Indeed both features, the mean-
field and the granularity peak are surface phenomena.
This fact can be easily read off from Fig. 1, since for the
respective pulse length the peaks are located near the
maximal energy contributed by surface ions. This is further
confirmed by comparing the mean-field spectra according
to Eq. (3) and the numerical ones from individual ions [19]
in Figs. 3(a)–3(c). Formally, these spectra correspond to
cuts at $T = 0$ in Fig. 1, but for different cluster sizes,
namely 100, 1000, and 10 000 atoms, respectively. One
sees that the spectrum deviates less from the mean-field
prediction for larger cluster size and correspondingly
smaller surface-to-volume ratio; nevertheless, the granu-
larity peak remains clearly visible.

That mean-field and granularity peak are of different
origin can be seen, e.g., from the formation of the maxima
in time: The mean-field peak builds up gradually in time
and appears toward the end of the explosion [Fig. 2(c)]
since inner shells of charge density need time to overtake
the outer ones. The granularity peak in the case of a short
pulse, on the other hand, appears right from the beginning
[Fig. 2(b)] suggesting that it can be understood from the
forces acting initially on the individual ions. This is indeed
the case as we will see.

Because of the repulsive interaction potential of the
atoms in the cluster, nearby particles are very unlikely in
the ground state. Hence, a correlation hole around an atom
or ion exists. This means if there is an atom at position $\mathbf{r}$ the
probability to find another atom at position $\mathbf{r}'$ within the
radius δ of the correlation hole, i.e., for $|\mathbf{r} - \mathbf{r}'| < \delta$,
vanishes leading to the characteristic pair-correlation func-
tion as shown in Fig. 3(d). It has been numerically obtained
by an ensemble average over

$$g(r) = \frac{R^3}{r^2 \tilde{g}(r)} \sum_{i \neq j} \delta(r - r_{ij}), \qquad (4)$$
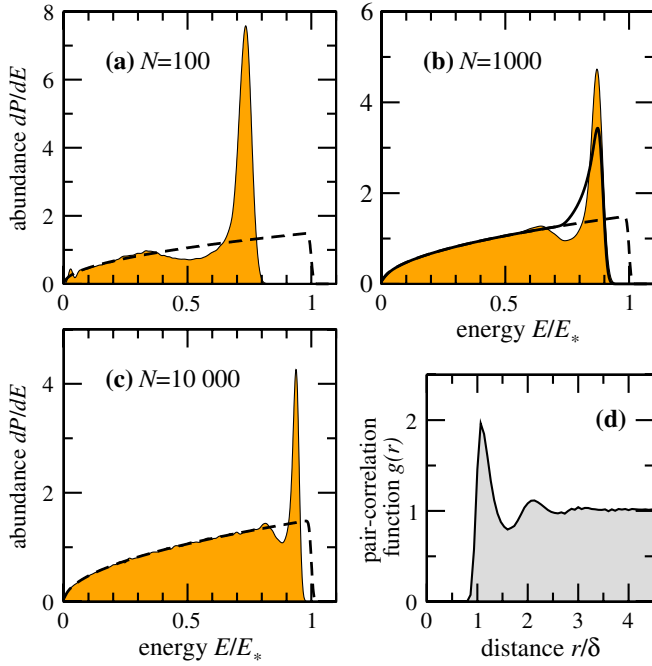
FIG. 3 (color online). Spectra from numerical propagation of systems with $N = 100$, 1000, and 10 000 ions, respectively, are shown by orange or gray-shaded areas (a)–(c). The mean-field model as given by Eq. (3) is shown with dashed lines. Considering a correlation hole in the mean-field description by using Eq. (8) in Eq. (2) yields the spectrum shown as solid line (b). Additionally the pair-correlation function $g(r)$ according to Eq. (4) is shown for the cluster with $N = 1000$ individual ions (d).

with r_{ij} the distance between the particles i and j and $\tilde{g}(r) = \frac{3}{16}(r/R - 2)^2(r/R + 4)$ the distribution of distances r in a sphere with radius R [20]. The normalization with $\tilde{g}(r)$ is necessary in order to remove the trivial dependence on r due to the finite size of the system.

We can assess how the correlation hole affects the force acting on an ion at position $\mathbf{r}$ analytically. To this end, we determine the Coulomb repulsion of the ion from an infinitesimally thin spherical shell of radius r' and charge q by integrating over all angles

$$\mathbf{f}_{r'}(\mathbf{r}) = \frac{q}{4\pi} \int_0^{2\pi} d\phi \int_0^{\pi} d\theta \sin\theta \frac{\partial}{\partial \mathbf{r}} \frac{1}{|\mathbf{r} - \mathbf{r}'|}, \quad (5)$$

with $\mathbf{r}' \equiv r'(\sin\theta\cos\phi, \sin\theta\sin\phi, \cos\theta)$ a vector on the shell. The radial component of this force can be determined without loss of generality by choosing $\mathbf{r} = r\hat{\mathbf{z}}$ along the z axis. Integrating over ϕ and using $\tau \equiv \cos\theta$ it reads

$$f_{r',\delta\tau}(r) = \frac{q}{2} \int_{-1}^{+1-\delta\tau} d\tau \frac{d}{dr} \frac{1}{\sqrt{r^2 + r'^2 - 2rr'\tau}}, \quad (6a)$$

$$= \frac{q}{r^2}\left[\frac{1}{2} + \frac{(1 - \delta\tau)r - r'}{2\sqrt{r'^2 + r^2 - 2(1 - \delta\tau)r'r}}\right]. \quad (6b)$$

Hereby, the integration was restricted to the upper limit $1 - \delta\tau < 1$ in order to account for a correlation hole, cf.

the sketch in Fig. 4 and its inset, which shows $\delta\tau$ explicitly. Equation (5) corresponds to $\delta\tau = 0$. In this case, performing the integration over τ yields—as expected—Gauss' law, i.e., $f_{r',0} = 0$ for $r < r'$ and $f_{r',0} = q/r^2$ for $r \geq r'$. As can be seen in Fig. 4(a), for finite $\delta\tau$ the force is $f_{r',\delta\tau} > 0$ inside the shell with radius r' and $f_{r',\delta\tau} < q/2r^2$ outside this shell. Yet, this modification of the forces does not play a role as long as the test particle's correlation hole is in the bulk ($r < R - \delta$, see test particle at r_1 in Fig. 4) since reduced repulsion from inner charged shells with $r' < r$ is fully compensated by a finite repulsion from outer shells with $r' > r$ in accordance with Gauss' law for spherical charge distributions and a test particle with its correlation sphere completely inside the charge distribution. A reduced force is expected at the surface (see test particle at r_2 in Fig. 4). Both expectations are confirmed by the cumulative force, i.e., the integration over all charged shells, shown in Fig. 4(b). For this integration we use $\delta\tau = (\delta^2 - (r - r')^2)/(2rr')$, which guarantees that the "open" shells (see thick green or gray line in the sketch of Fig. 4) form a spherical correlation hole with radius δ for $|r - r'| \leq \delta$. For all other shells it is $\delta\tau = 0$. This $\delta\tau$ inserted into Eq. (6) and integrated over all shells yields an explicit expression for the force in the presence of a correlation hole
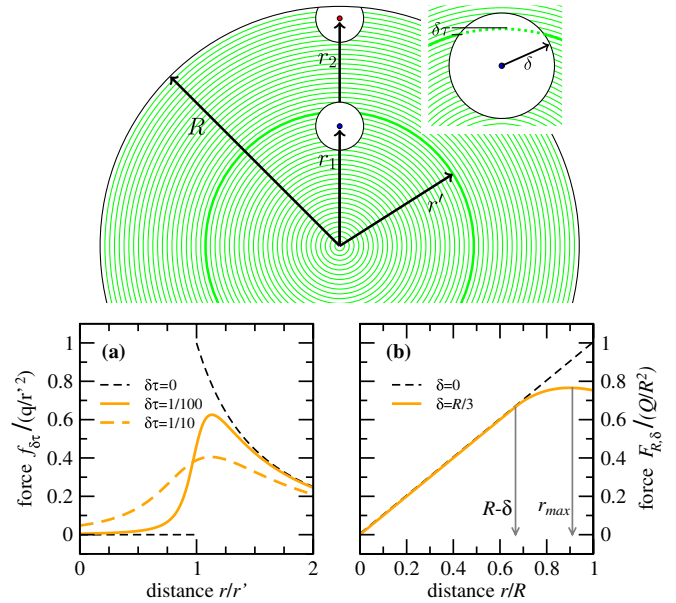
FIG. 4 (color online). Sketch of the integration assuming a correlation hole with radius δ around the test particle at distance r. We show two situations, where the correlation hole is inside the bulk (r_1) and at the surface (r_2), respectively. The test particle force is obtained by integration over all shells (indicated by green or gray lines) with some of them being "open" (thick green or gray line, see also inset) due to the correlation hole. The force on a test particle as a function of the distance r (a) due to an "open" charged spherical shell with radius r according to Eq. (6) and (b) integrated over all shells of the charged sphere of radius R according to Eq. (7).

$$F_{R,\delta}(r) = Qr/R^3 \quad \text{for } r < R - \delta \tag{7a}$$

$$= A_{R,\delta}(r)Qr/R^3 \quad \text{for } R - \delta < r < R, \tag{7b}$$

with the dimensionless attenuation factor

$$A_{R,\delta}(r) \equiv \frac{(r + R - \delta)^2(2(r+R)\delta + \delta^2 - 3(r-R)^2)}{16\delta r^3}. \tag{7c}$$

Indeed, the force from Eq. (7) increases linearly, characteristic for a homogeneously charged sphere and without any effect of the correlation hole until the latter touches the surface from the inside [for the case shown in Fig. 4(b) at $r = 2R/3$]. When this happens the force grows more slowly than in the homogeneous case and even decreases still within the charged sphere reaching a maximal value at $r_{\max} = R - \delta/3$ (for $\delta \ll R$).

With the initial forces sculpturing the properties of the final ion-energy spectrum, we may even attempt to calculate this spectrum according to Eq. (2). We assume a self-similar expansion, i.e., scaling of all lengths in the system with the common factor η. Consequently, the force (7) inherits the property $F_{\eta R, \eta\delta}(\eta r) = \eta^{-2}F_{R,\delta}(r)$ from the Coulomb force. Thus, the final kinetic energy depends on the initial position similarly as in the case of a homogenous charge density through an integral along the similarity path with increment $dr' = rd\eta$

$$E(r) = r\int_1^\infty d\eta F_{\eta R, \eta\delta}(\eta r) = rF_{R,\delta}(r). \tag{8}$$

In all (numerical and analytical) spectra presented we take into account a finite energy resolution $\delta E = E_\star/50$. For Eq. (2) this means to replace $\delta(x)$ with $K_{\delta E}(x) = \exp(-(x/\delta E)^2)/\sqrt{\pi}\delta E$. In Fig. 3(b) one sees the spectrum for clusters with 1000 atoms in comparison to the one obtained with the mean-field approach including the correlation hole as just described. The deviations of both the numerical result (orange or gray-shaded area) and the correlation-hole result (solid line) with respect to the simple mean-field result (dashed line) from Eq. (3) at energies $E \lesssim E_\star$ clearly reveals the importance of the correlation hole.

However, given the analytically calculated force of Eq. (7b) we also know that in order for the correlation hole to have an effect, the ion density must have a sharp edge, essentially falling to zero within the radius δ of the correlation hole. Otherwise, the forces of each shell in the presence of the correlation hole will compensate each other; see Fig. 4(a). On the other hand, a soft edge gives rise to the mean-field peak through catching up of faster inner ions with the slower outer ones, as described in the introduction. We may quantitatively describe the edge by a Fermi distribution $\varrho_{a,R}(r) = 2\tilde{\varrho}_{a,R}/[1 + \exp((r - R)/a)]$ with the softness parameter a and $\tilde{\varrho}_{a,R}$ the ion density at $r = R$ which is determined through the integral $4\pi \int dr r^2 \varrho_{a,R}(r) = N$. In Fig. 5 the energy spectrum of ions initially distributed according to a Fermi distribution $\varrho_{a,R}(r)$ is shown for various values of a measured in terms
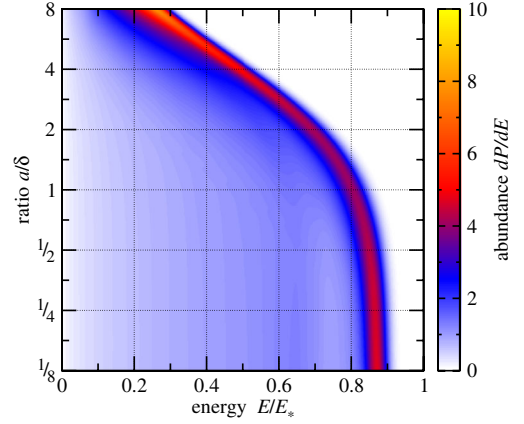
FIG. 5 (color online). Energy spectra as obtained from an exploding cluster with 1000 particles for various cluster edges a (implemented with Fermi distribution function, see text), which is given in units of the correlation hole radius δ. Energy is given in terms of $E_\star$, cf. Eq. (3b).

of the correlation hole radius δ. One can see the crossover from the granularity to the mean-field peak near $a = \delta$.

We have seen that these two features are of very different origins, although both of them are surface effects and occur, therefore, on the rim of maximal energy in the spectra of Fig. 5. It should be possible in an experiment to reveal both phenomena and their crossover by simply varying the pulse length of the ionizing light pulse as demonstrated in Fig. 1. A time-delayed probe pulse could reveal, in addition, the different temporal behavior of both peaks illustrated in Fig. 2.

In the examples discussed here, the granularity of the system was quantified by the correlation hole which is the most common case for ground state matter. However, a little thought reveals that ions (or electrons) randomly distributed over a finite volume give rise to a granularity peak as well. It is much weaker and broader [21] but still has the same reason: Forces on an ion from other ions inside and outside a virtual shell do not compensate each other near the edge of the sample where the radius of the shell is defined by the distance of the ion to the charge center of the sample.

*Present address: Institute of Integrative Biology, ETH Zurich, Universitätstraße 16, 8092 Zurich, Switzerland.
[1] P. Fulde, *Electron Correlations in Molecules and Solids* (Springer, Heidelberg, 1995).
[2] B. W. J. McNeil and N. R. Thompson, Nat. Photonics **4**, 814 (2010).
[3] P. Emma *et al.*, Nat. Photonics **4**, 641 (2010).
[4] C. Gnodtke, U. Saalmann, and J. M. Rost, Phys. Rev. Lett. **108**, 175003 (2012).

[5] C. Gnodtke, U. Saalmann, and J.-M. Rost, Chem. Phys. **414,** 65 (2013).

[6] T. Gorkhover *et al.*, Phys. Rev. Lett. **108,** 245005 (2012).

[7] H. Thomas *et al.*, Phys. Rev. Lett. **108,** 133401 (2012).

[8] S. Schorb *et al.*, Phys. Rev. Lett. **108,** 233401 (2012).

[9] U. Saalmann and J. M. Rost, Phys. Rev. Lett. **89,** 143401 (2002).

[10] Because of Gauss' law this is just the time it would take two charges Q with reduced mass M to double their (initial) distance R [11].

[11] L. D. Landau and E. M. Lifschitz, *Mechanics* (Pergamon Press, Oxford, 1994).

[12] K. Nishihara, H. Amitani, M. Murakami, S. V. Bulanov, and T. Z. Esirkepov, Nucl. Instrum. Methods Phys. Res., Sect. A **464,** 98 (2001).

[13] A. E. Kaplan, B. Y. Dubetsky, and P. L. Shkolnikov, Phys. Rev. Lett. **91,** 143401 (2003).

[14] Md. R. Islam, U. Saalmann, and J. M. Rost, Phys. Rev. A **73,** 041201(R) (2006).

[15] LJ clusters imply that the ground state configuration of those clusters is obtained by minimizing the LJ interaction between the atoms. Starting from this configuration we perform a 3D-molecular-dynamics propagation until we obtain converged energies for the exploding ions.

[16] C. Gnodtke, U. Saalmann, and J. M. Rost, New J. Phys. **13,** 013028 (2011).

[17] V. F. Kovalev and V. Y. Bychenkov, JETP **101,** 212 (2005); V. Y. Bychenkov and V. F. Kovalev, Plasma Phys. Rep. **31,** 178 (2005).

[18] F. Peano, R. A. Fonseca, and L. O. Silva, Phys. Rev. Lett. **94,** 033401 (2005).

[19] The ions have been placed radially on equal-volume shells guaranteeing that the resulting granular density approximates the homogeneous density as close as possible. The angular positions of the ions are relaxed to minimize their interaction energy given by mutual LJ potentials.

[20] R. García-Pelayo, J. Phys. A **38,** 3475 (2005).

[21] U. Saalmann, A. Mikaberidze, and J. M. Rost (unpublished).